BABAR-PUB-07/060
SLAC-PUB-12818

Study of the Exclusive Initial-State-Radiation Production of the $D\overline{D}$ System.

B. Aubert,[1] M. Bona,[1] D. Boutigny,[1] Y. Karyotakis,[1] J. P. Lees,[1] V. Poireau,[1] X. Prudent,[1] V. Tisserand,[1] A. Zghiche,[1] J. Garra Tico,[2] E. Grauges,[2] L. Lopez,[3] A. Palano,[3] M. Pappagallo,[3] G. Eigen,[4] B. Stugu,[4] L. Sun,[4] G. S. Abrams,[5] M. Battaglia,[5] D. N. Brown,[5] J. Button-Shafer,[5] R. N. Cahn,[5] Y. Groysman,[5] R. G. Jacobsen,[5] J. A. Kadyk,[5] L. T. Kerth,[5] Yu. G. Kolomensky,[5] G. Kukartsev,[5] D. Lopes Pegna,[5] G. Lynch,[5] L. M. Mir,[5] T. J. Orimoto,[5] I. L. Osipenkov,[5] M. T. Ronan,[5,*] K. Tackmann,[5] T. Tanabe,[5] W. A. Wenzel,[5] P. del Amo Sanchez,[6] C. M. Hawkes,[6] A. T. Watson,[6] H. Koch,[7] T. Schroeder,[7] D. Walker,[8] D. J. Asgeirsson,[9] T. Cuhadar-Donszelmann,[9] B. G. Fulsom,[9] C. Hearty,[9] T. S. Mattison,[9] J. A. McKenna,[9] M. Barrett,[10] A. Khan,[10] M. Saleem,[10] L. Teodorescu,[10] V. E. Blinov,[11] A. D. Bukin,[11] V. P. Druzhinin,[11] V. B. Golubev,[11] A. P. Onuchin,[11] S. I. Serednyakov,[11] Yu. I. Skovpen,[11] E. P. Solodov,[11] K. Yu. Todyshev,[11] M. Bondioli,[12] S. Curry,[12] I. Eschrich,[12] D. Kirkby,[12] A. J. Lankford,[12] P. Lund,[12] M. Mandelkern,[12] E. C. Martin,[12] D. P. Stoker,[12] S. Abachi,[13] C. Buchanan,[13] S. D. Foulkes,[14] J. W. Gary,[14] F. Liu,[14] O. Long,[14] B. C. Shen,[14] G. M. Vitug,[14] L. Zhang,[14] H. P. Paar,[15] S. Rahatlou,[15] V. Sharma,[15] J. W. Berryhill,[16] C. Campagnari,[16] A. Cunha,[16] B. Dahmes,[16] T. M. Hong,[16] D. Kovalskyi,[16] J. D. Richman,[16] T. W. Beck,[17] A. M. Eisner,[17] C. J. Flacco,[17] C. A. Heusch,[17] J. Kroseberg,[17] W. S. Lockman,[17] T. Schalk,[17] B. A. Schumm,[17] A. Seiden,[17] M. G. Wilson,[17] L. O. Winstrom,[17] E. Chen,[18] C. H. Cheng,[18] F. Fang,[18] D. G. Hitlin,[18] I. Narsky,[18] T. Piatenko,[18] F. C. Porter,[18] R. Andreassen,[19] G. Mancinelli,[19] B. T. Meadows,[19] K. Mishra,[19] M. D. Sokoloff,[19] F. Blanc,[20] P. C. Bloom,[20] S. Chen,[20] W. T. Ford,[20] J. F. Hirschauer,[20] A. Kreisel,[20] M. Nagel,[20] U. Nauenberg,[20] A. Olivas,[20] J. G. Smith,[20] K. A. Ulmer,[20] S. R. Wagner,[20] J. Zhang,[20] A. M. Gabareen,[21] A. Soffer,[21,†] W. H. Toki,[21] R. J. Wilson,[21] F. Winklmeier,[21] D. D. Altenburg,[22] E. Feltresi,[22] A. Hauke,[22] H. Jasper,[22] J. Merkel,[22] A. Petzold,[22] B. Spaan,[22] K. Wacker,[22] V. Klose,[23] M. J. Kobel,[23] H. M. Lacker,[23] W. F. Mader,[23] R. Nogowski,[23] J. Schubert,[23] K. R. Schubert,[23] R. Schwierz,[23] J. E. Sundermann,[23] A. Volk,[23] D. Bernard,[24] G. R. Bonneaud,[24] E. Latour,[24] V. Lombardo,[24] Ch. Thiebaux,[24] M. Verderi,[24] P. J. Clark,[25] W. Gradl,[25] F. Muheim,[25] S. Playfer,[25] A. I. Robertson,[25] J. E. Watson,[25] Y. Xie,[25] M. Andreotti,[26] D. Bettoni,[26] C. Bozzi,[26] R. Calabrese,[26] A. Cecchi,[26] G. Cibinetto,[26] P. Franchini,[26] E. Luppi,[26] M. Negrini,[26] A. Petrella,[26] L. Piemontese,[26] E. Prencipe,[26] V. Santoro,[26] F. Anulli,[27] R. Baldini-Ferroli,[27] A. Calcaterra,[27] R. de Sangro,[27] G. Finocchiaro,[27] S. Pacetti,[27] P. Patteri,[27] I. M. Peruzzi,[27,‡] M. Piccolo,[27] M. Rama,[27] A. Zallo,[27] A. Buzzo,[28] R. Contri,[28] M. Lo Vetere,[28] M. M. Macri,[28] M. R. Monge,[28] S. Passaggio,[28] C. Patrignani,[28] E. Robutti,[28] A. Santroni,[28] S. Tosi,[28] K. S. Chaisanguanthum,[29] M. Morii,[29] J. Wu,[29] R. S. Dubitzky,[30] J. Marks,[30] S. Schenk,[30] U. Uwer,[30] D. J. Bard,[31] P. D. Dauncey,[31] R. L. Flack,[31] J. A. Nash,[31] W. Panduro Vazquez,[31] M. Tibbetts,[31] P. K. Behera,[32] X. Chai,[32] M. J. Charles,[32] U. Mallik,[32] J. Cochran,[33] H. B. Crawley,[33] L. Dong,[33] V. Eyges,[33] W. T. Meyer,[33] S. Prell,[33] E. I. Rosenberg,[33] A. E. Rubin,[33] Y. Y. Gao,[34] A. V. Gritsan,[34] Z. J. Guo,[34] C. K. Lae,[34] A. G. Denig,[35] M. Fritsch,[35] G. Schott,[35] N. Arnaud,[36] J. Béquilleux,[36] A. D'Orazio,[36] M. Davier,[36] G. Grosdidier,[36] A. Höcker,[36] V. Lepeltier,[36] F. Le Diberder,[36] A. M. Lutz,[36] S. Pruvot,[36] S. Rodier,[36] P. Roudeau,[36] M. H. Schune,[36] J. Serrano,[36] V. Sordini,[36] A. Stocchi,[36] W. F. Wang,[36] G. Wormser,[36] D. J. Lange,[37] D. M. Wright,[37] I. Bingham,[38] J. P. Burke,[38] C. A. Chavez,[38] J. R. Fry,[38] E. Gabathuler,[38] R. Gamet,[38] D. E. Hutchcroft,[38] D. J. Payne,[38] K. C. Schofield,[38] C. Touramanis,[38] A. J. Bevan,[39] K. A. George,[39] F. Di Lodovico,[39] R. Sacco,[39] G. Cowan,[40] H. U. Flaecher,[40] D. A. Hopkins,[40] S. Paramesvaran,[40] F. Salvatore,[40] A. C. Wren,[40] D. N. Brown,[41] C. L. Davis,[41] J. Allison,[42] D. Bailey,[42] N. R. Barlow,[42] R. J. Barlow,[42] Y. M. Chia,[42] C. L. Edgar,[42] G. D. Lafferty,[42] T. J. West,[42] J. I. Yi,[42] J. Anderson,[43] C. Chen,[43] A. Jawahery,[43] D. A. Roberts,[43] G. Simi,[43] J. M. Tuggle,[43] G. Blaylock,[44] C. Dallapiccola,[44] S. S. Hertzbach,[44] X. Li,[44] T. B. Moore,[44] E. Salvati,[44] S. Saremi,[44] R. Cowan,[45] D. Dujmic,[45] P. H. Fisher,[45] K. Koeneke,[45] G. Sciolla,[45] M. Spitznagel,[45] F. Taylor,[45] R. K. Yamamoto,[45] M. Zhao,[45] Y. Zheng,[45] S. E. Mclachlin,[46,*] P. M. Patel,[46] S. H. Robertson,[46] A. Lazzaro,[47] F. Palombo,[47] J. M. Bauer,[48] L. Cremaldi,[48] V. Eschenburg,[48] R. Godang,[48] R. Kroeger,[48] D. A. Sanders,[48] D. J. Summers,[48] H. W. Zhao,[48] S. Brunet,[49] D. Côté,[49] M. Simard,[49] P. Taras,[49] F. B. Viaud,[49] H. Nicholson,[50] G. De Nardo,[51] F. Fabozzi,[51,§] L. Lista,[51] D. Monorchio,[51] C. Sciacca,[51] M. A. Baak,[52] G. Raven,[52] H. L. Snoek,[52] C. P. Jessop,[53] K. J. Knoepfel,[53] J. M. LoSecco,[53] G. Benelli,[54] L. A. Corwin,[54] K. Honscheid,[54] H. Kagan,[54] R. Kass,[54] J. P. Morris,[54] A. M. Rahimi,[54] J. J. Regensburger,[54] S. J. Sekula,[54] Q. K. Wong,[54] N. L. Blount,[55] J. Brau,[55] R. Frey,[55] O. Igonkina,[55] J. A. Kolb,[55] M. Lu,[55] R. Rahmat,[55] N. B. Sinev,[55] D. Strom,[55] J. Strube,[55] E. Torrence,[55] N. Gagliardi,[56] A. Gaz,[56] M. Margoni,[56] M. Morandin,[56] A. Pompili,[56] M. Posocco,[56] M. Rotondo,[56]

F. Simonetto,[56] R. Stroili,[56] C. Voci,[56] E. Ben-Haim,[57] H. Briand,[57] G. Calderini,[57] J. Chauveau,[57] P. David,[57] L. Del Buono,[57] Ch. de la Vaissière,[57] O. Hamon,[57] Ph. Leruste,[57] J. Malclès,[57] J. Ocariz,[57] A. Perez,[57] J. Prendki,[57] L. Gladney,[58] M. Biasini,[59] R. Covarelli,[59] E. Manoni,[59] C. Angelini,[60] G. Batignani,[60] S. Bettarini,[60] M. Carpinelli,[60] R. Cenci,[60] A. Cervelli,[60] F. Forti,[60] M. A. Giorgi,[60] A. Lusiani,[60] G. Marchiori,[60] M. A. Mazur,[60] M. Morganti,[60] N. Neri,[60] E. Paoloni,[60] G. Rizzo,[60] J. J. Walsh,[60] J. Biesiada,[61] P. Elmer,[61] Y. P. Lau,[61] C. Lu,[61] J. Olsen,[61] A. J. S. Smith,[61] A. V. Telnov,[61] E. Baracchini,[62] F. Bellini,[62] G. Cavoto,[62] D. del Re,[62] E. Di Marco,[62] R. Faccini,[62] F. Ferrarotto,[62] F. Ferroni,[62] M. Gaspero,[62] P. D. Jackson,[62] L. Li Gioi,[62] M. A. Mazzoni,[62] S. Morganti,[62] G. Piredda,[62] F. Polci,[62] F. Renga,[62] C. Voena,[62] M. Ebert,[63] T. Hartmann,[63] H. Schröder,[63] R. Waldi,[63] T. Adye,[64] G. Castelli,[64] B. Franek,[64] E. O. Olaiya,[64] W. Roethel,[64] F. F. Wilson,[64] S. Emery,[65] M. Escalier,[65] A. Gaidot,[65] S. F. Ganzhur,[65] G. Hamel de Monchenault,[65] W. Kozanecki,[65] G. Vasseur,[65] Ch. Yèche,[65] M. Zito,[65] X. R. Chen,[66] H. Liu,[66] W. Park,[66] M. V. Purohit,[66] R. M. White,[66] J. R. Wilson,[66] M. T. Allen,[67] D. Aston,[67] R. Bartoldus,[67] P. Bechtle,[67] R. Claus,[67] J. P. Coleman,[67] M. R. Convery,[67] J. C. Dingfelder,[67] J. Dorfan,[67] G. P. Dubois-Felsmann,[67] W. Dunwoodie,[67] R. C. Field,[67] T. Glanzman,[67] S. J. Gowdy,[67] M. T. Graham,[67] P. Grenier,[67] C. Hast,[67] W. R. Innes,[67] J. Kaminski,[67] M. H. Kelsey,[67] H. Kim,[67] P. Kim,[67] M. L. Kocian,[67] D. W. G. S. Leith,[67] S. Li,[67] S. Luitz,[67] V. Luth,[67] H. L. Lynch,[67] D. B. MacFarlane,[67] H. Marsiske,[67] R. Messner,[67] D. R. Muller,[67] C. P. O'Grady,[67] I. Ofte,[67] A. Perazzo,[67] M. Perl,[67] T. Pulliam,[67] B. N. Ratcliff,[67] A. Roodman,[67] A. A. Salnikov,[67] R. H. Schindler,[67] J. Schwiening,[67] A. Snyder,[67] D. Su,[67] M. K. Sullivan,[67] K. Suzuki,[67] S. K. Swain,[67] J. M. Thompson,[67] J. Va'vra,[67] A. P. Wagner,[67] M. Weaver,[67] W. J. Wisniewski,[67] M. Wittgen,[67] D. H. Wright,[67] A. K. Yarritu,[67] K. Yi,[67] C. C. Young,[67] V. Ziegler,[67] P. R. Burchat,[68] A. J. Edwards,[68] S. A. Majewski,[68] T. S. Miyashita,[68] B. A. Petersen,[68] L. Wilden,[68] S. Ahmed,[69] M. S. Alam,[69] R. Bula,[69] J. A. Ernst,[69] V. Jain,[69] B. Pan,[69] M. A. Saeed,[69] F. R. Wappler,[69] S. B. Zain,[69] M. Krishnamurthy,[70] S. M. Spanier,[70] R. Eckmann,[71] J. L. Ritchie,[71] A. M. Ruland,[71] C. J. Schilling,[71] R. F. Schwitters,[71] J. M. Izen,[72] X. C. Lou,[72] S. Ye,[72] F. Bianchi,[73] F. Gallo,[73] D. Gamba,[73] M. Pelliccioni,[73] M. Bomben,[74] L. Bosisio,[74] C. Cartaro,[74] F. Cossutti,[74] G. Della Ricca,[74] L. Lanceri,[74] L. Vitale,[74] V. Azzolini,[75] N. Lopez-March,[75] F. Martinez-Vidal,[75,¶] D. A. Milanes,[75] A. Oyanguren,[75] J. Albert,[76] Sw. Banerjee,[76] B. Bhuyan,[76] K. Hamano,[76] R. Kowalewski,[76] I. M. Nugent,[76] J. M. Roney,[76] R. J. Sobie,[76] P. F. Harrison,[77] J. Ilic,[77] T. E. Latham,[77] G. B. Mohanty,[77] H. R. Band,[78] X. Chen,[78] S. Dasu,[78] K. T. Flood,[78] J. J. Hollar,[78] P. E. Kutter,[78] Y. Pan,[78] M. Pierini,[78] R. Prepost,[78] S. L. Wu,[78] and H. Neal[79]

(The *BABAR* Collaboration)

[1]*Laboratoire de Physique des Particules, IN2P3/CNRS et Université de Savoie, F-74941 Annecy-Le-Vieux, France*
[2]*Universitat de Barcelona, Facultat de Fisica, Departament ECM, E-08028 Barcelona, Spain*
[3]*Università di Bari, Dipartimento di Fisica and INFN, I-70126 Bari, Italy*
[4]*University of Bergen, Institute of Physics, N-5007 Bergen, Norway*
[5]*Lawrence Berkeley National Laboratory and University of California, Berkeley, California 94720, USA*
[6]*University of Birmingham, Birmingham, B15 2TT, United Kingdom*
[7]*Ruhr Universität Bochum, Institut für Experimentalphysik 1, D-44780 Bochum, Germany*
[8]*University of Bristol, Bristol BS8 1TL, United Kingdom*
[9]*University of British Columbia, Vancouver, British Columbia, Canada V6T 1Z1*
[10]*Brunel University, Uxbridge, Middlesex UB8 3PH, United Kingdom*
[11]*Budker Institute of Nuclear Physics, Novosibirsk 630090, Russia*
[12]*University of California at Irvine, Irvine, California 92697, USA*
[13]*University of California at Los Angeles, Los Angeles, California 90024, USA*
[14]*University of California at Riverside, Riverside, California 92521, USA*
[15]*University of California at San Diego, La Jolla, California 92093, USA*
[16]*University of California at Santa Barbara, Santa Barbara, California 93106, USA*
[17]*University of California at Santa Cruz, Institute for Particle Physics, Santa Cruz, California 95064, USA*
[18]*California Institute of Technology, Pasadena, California 91125, USA*
[19]*University of Cincinnati, Cincinnati, Ohio 45221, USA*
[20]*University of Colorado, Boulder, Colorado 80309, USA*
[21]*Colorado State University, Fort Collins, Colorado 80523, USA*
[22]*Universität Dortmund, Institut für Physik, D-44221 Dortmund, Germany*
[23]*Technische Universität Dresden, Institut für Kern- und Teilchenphysik, D-01062 Dresden, Germany*
[24]*Laboratoire Leprince-Ringuet, CNRS/IN2P3, Ecole Polytechnique, F-91128 Palaiseau, France*
[25]*University of Edinburgh, Edinburgh EH9 3JZ, United Kingdom*
[26]*Università di Ferrara, Dipartimento di Fisica and INFN, I-44100 Ferrara, Italy*
[27]*Laboratori Nazionali di Frascati dell'INFN, I-00044 Frascati, Italy*

[28] Università di Genova, Dipartimento di Fisica and INFN, I-16146 Genova, Italy
[29] Harvard University, Cambridge, Massachusetts 02138, USA
[30] Universität Heidelberg, Physikalisches Institut, Philosophenweg 12, D-69120 Heidelberg, Germany
[31] Imperial College London, London, SW7 2AZ, United Kingdom
[32] University of Iowa, Iowa City, Iowa 52242, USA
[33] Iowa State University, Ames, Iowa 50011-3160, USA
[34] Johns Hopkins University, Baltimore, Maryland 21218, USA
[35] Universität Karlsruhe, Institut für Experimentelle Kernphysik, D-76021 Karlsruhe, Germany
[36] Laboratoire de l'Accélérateur Linéaire, IN2P3/CNRS et Université Paris-Sud 11, Centre Scientifique d'Orsay, B. P. 34, F-91898 ORSAY Cedex, France
[37] Lawrence Livermore National Laboratory, Livermore, California 94550, USA
[38] University of Liverpool, Liverpool L69 7ZE, United Kingdom
[39] Queen Mary, University of London, E1 4NS, United Kingdom
[40] University of London, Royal Holloway and Bedford New College, Egham, Surrey TW20 0EX, United Kingdom
[41] University of Louisville, Louisville, Kentucky 40292, USA
[42] University of Manchester, Manchester M13 9PL, United Kingdom
[43] University of Maryland, College Park, Maryland 20742, USA
[44] University of Massachusetts, Amherst, Massachusetts 01003, USA
[45] Massachusetts Institute of Technology, Laboratory for Nuclear Science, Cambridge, Massachusetts 02139, USA
[46] McGill University, Montréal, Québec, Canada H3A 2T8
[47] Università di Milano, Dipartimento di Fisica and INFN, I-20133 Milano, Italy
[48] University of Mississippi, University, Mississippi 38677, USA
[49] Université de Montréal, Physique des Particules, Montréal, Québec, Canada H3C 3J7
[50] Mount Holyoke College, South Hadley, Massachusetts 01075, USA
[51] Università di Napoli Federico II, Dipartimento di Scienze Fisiche and INFN, I-80126, Napoli, Italy
[52] NIKHEF, National Institute for Nuclear Physics and High Energy Physics, NL-1009 DB Amsterdam, The Netherlands
[53] University of Notre Dame, Notre Dame, Indiana 46556, USA
[54] Ohio State University, Columbus, Ohio 43210, USA
[55] University of Oregon, Eugene, Oregon 97403, USA
[56] Università di Padova, Dipartimento di Fisica and INFN, I-35131 Padova, Italy
[57] Laboratoire de Physique Nucléaire et de Hautes Energies, IN2P3/CNRS, Université Pierre et Marie Curie-Paris6, Université Denis Diderot-Paris7, F-75252 Paris, France
[58] University of Pennsylvania, Philadelphia, Pennsylvania 19104, USA
[59] Università di Perugia, Dipartimento di Fisica and INFN, I-06100 Perugia, Italy
[60] Università di Pisa, Dipartimento di Fisica, Scuola Normale Superiore and INFN, I-56127 Pisa, Italy
[61] Princeton University, Princeton, New Jersey 08544, USA
[62] Università di Roma La Sapienza, Dipartimento di Fisica and INFN, I-00185 Roma, Italy
[63] Universität Rostock, D-18051 Rostock, Germany
[64] Rutherford Appleton Laboratory, Chilton, Didcot, Oxon, OX11 0QX, United Kingdom
[65] DSM/Dapnia, CEA/Saclay, F-91191 Gif-sur-Yvette, France
[66] University of South Carolina, Columbia, South Carolina 29208, USA
[67] Stanford Linear Accelerator Center, Stanford, California 94309, USA
[68] Stanford University, Stanford, California 94305-4060, USA
[69] State University of New York, Albany, New York 12222, USA
[70] University of Tennessee, Knoxville, Tennessee 37996, USA
[71] University of Texas at Austin, Austin, Texas 78712, USA
[72] University of Texas at Dallas, Richardson, Texas 75083, USA
[73] Università di Torino, Dipartimento di Fisica Sperimentale and INFN, I-10125 Torino, Italy
[74] Università di Trieste, Dipartimento di Fisica and INFN, I-34127 Trieste, Italy
[75] IFIC, Universitat de Valencia-CSIC, E-46071 Valencia, Spain
[76] University of Victoria, Victoria, British Columbia, Canada V8W 3P6
[77] Department of Physics, University of Warwick, Coventry CV4 7AL, United Kingdom
[78] University of Wisconsin, Madison, Wisconsin 53706, USA
[79] Yale University, New Haven, Connecticut 06511, USA

(Dated: November 14, 2007)

A search for charmonium and other new states is performed in a study of exclusive initial-state-radiation production of $D\overline{D}$ events from electron-positron annihilations at a center-of-mass energy of 10.58 GeV. The data sample corresponds to an integrated luminosity of 384 fb^{-1} and was recorded by the *BABAR* experiment at the PEP-II storage ring. The $D\overline{D}$ mass spectrum shows clear evidence of the $\psi(3770)$ plus other structures near 3.9, 4.1, and 4.4 GeV/c^2. No evidence for $Y(4260) \to D\overline{D}$ is observed, leading to an upper limit of $\mathcal{B}(Y(4260) \to D\overline{D})/\mathcal{B}(Y(4260) \to J/\psi\pi^+\pi^-) < 1.0$ at 90% confidence level.

PACS numbers: 13.66.Bc, 13.87.Fh, 14.40.Gx

The surprising discovery of new states decaying to $J/\psi\pi^+\pi^-$ [1, 2] has renewed interest in the field of charmonium spectroscopy, as the new states are not easy to accommodate in the quark model. In particular, the *BABAR* experiment has discovered a new broad state, $Y(4260)$, decaying to $J/\psi\pi^+\pi^-$ in the initial-state-radiation (ISR) reaction $e^+e^- \to \gamma_{ISR}Y(4260)$. The quantum numbers $J^{PC} = 1^{--}$ are inferred from the single virtual-photon production mechanism. Structure, possibly related to the $Y(4260)$, has been observed in the reaction $e^+e^- \to \gamma_{ISR}\psi(2S)\pi^+\pi^-$ [3]. A charmonium state at this mass would be expected to decay predominantly to $D\overline{D}$, $D\overline{D}^*$ or $D^*\overline{D}^*$ [4]. It is peculiar that the decay rate to the hidden charm final state $J/\psi\pi^+\pi^-$ is much larger for the $Y(4260)$ than for excited charmonium states [5], and that at the $Y(4260)$ mass the cross section for $e^+e^- \to$ hadrons exhibits a local minimum [6]. Many theoretical interpretations for the $Y(4260)$ have been proposed, including unconventional scenarios: quark-antiquark gluon hybrids [7], tetraquarks [8] and hadronic molecules [9]. For a discussion and a list of references see, for example, Ref. [10].

This work explores ISR production of the $D\overline{D}$ final state for evidence of charmonium states and unconventional structures. A study by the BELLE collaboration of the $D\overline{D}^*$, and $D^*\overline{D}^*$ final states can be found in Ref. [11].

This analysis is based on a 384 fb^{-1} data sample recorded at the $\Upsilon(4S)$ resonance and 40 MeV/c^2 below the resonance by the *BABAR* detector at the PEP-II asymmetric-energy e^+e^- storage rings. The *BABAR* detector is described in detail elsewhere [12]. Charged particles are detected and their momenta measured by a combination of a cylindrical drift chamber (DCH) and a silicon vertex tracker (SVT), both operating within a 1.5-T magnetic field of a superconducting solenoid. A ring-imaging Cherenkov detector (DIRC) combined with energy-loss measurements in the SVT and DCH are used to identify charged kaon and pion candidates. Photon energies are measured with a CsI(Tl) electromagnetic calorimeter (EMC).

$D\overline{D}$ candidates are reconstructed in seven combinations of D decay modes, listed in Table I [13]. In each channel we allow any number of photons in the event. Events are selected if the number of well-measured tracks is exactly equal to the total number of charged daughter particles for the D and the $\overline{D}$ final states. Neutral pion candidates are formed from pairs of photons each having an energy greater than 30 MeV. The K^0_S candidates are reconstructed in the $\pi^+\ \pi^-$ decay mode. The tracks of each D candidate are geometrically constrained to come from a common vertex. Additionally, for the $D^0 \to K^-\pi^+\pi^0$ channel, π^0 and D^0 mass constraints are included in the fit, and for the $D^- \to K^0_S\pi^-$ channel a K^0_S mass constraint is imposed. D candidates with a χ^2 fit probability greater than 0.1% are retained. Subsequently, each $D\overline{D}$ pair is refitted to a common vertex with the constraint that they originate from the e^+e^- interaction region; only candidates with a χ^2 fit probability greater than 0.1% are retained. Extra π^0 candidates may originate from random combinations of photons. Aside from π^0's from D^0 decays, we require that there be no more than one other π^0 candidate in the event (except for channel 4, where we require that there are none).

For D channels without a π^0 candidate, the D momentum is determined from the summed 3-momenta of the decay particles and the energy is computed using the nominal D mass value [6, 14]. For the $D^0 \to K^-\pi^+\pi^0$ channel, the 4-momentum from the mass constrained fit is used. This procedure gives similar $D\overline{D}$ mass resolutions for all the channels.

The ISR photon, preferentially emitted at small angles with respect to the beam axis, escapes detection in approximately 90% of events. We therefore reconstruct the ISR photon as a missing particle. We define the squared recoil mass (M^2_{rec}) to the $D\overline{D}$ system using the four-momenta of the beam particles ($p_{e^\pm}$) and the reconstructed D (p_D) and $\overline{D}$ ($p_{\overline{D}}$):

$$M^2_{rec} \equiv (p_{e^-} + p_{e^+} - p_D - p_{\overline{D}})^2. \qquad (1)$$

This quantity should peak near zero for ISR events and for exclusive production of $e^+e^- \to D\overline{D}$ or $e^+e^- \to D\overline{D}^*$. In the latter case, the $D\overline{D}$ mass distribution peaks at masses well above 6 GeV/c^2. Therefore we select ISR events by requiring a $D\overline{D}$ invariant mass below 6 GeV/c^2 and $\mid M^2_{rec} \mid < 1$ GeV$^2/c^4$.

Monte Carlo simulations of $e^+e^- \to \gamma_{ISR}D\overline{D}$ and candidates from the process $e^+e^- \to \gamma_{ISR}J/\psi$, $J/\psi \to K^+K^-\pi^+\pi^-$ in data are used to validate the requirement on the number of residual π^0 and the shape of the M^2_{rec} distribution.

To estimate the number of background events in the signal region, the two-dimensional space spanned by the invariant masses of the two D candidates in each event is divided into nine regions: a central signal region and eight sideband regions above and below the signal regions, as illustrated in Fig. 1 for $D\overline{D}$ candidates reconstructed for the case of the $K^-\pi^+$ and $K^+\pi^-$ modes. The mass range for the signal region is within $\pm 2.5\sigma$ of the D mass, and the sideband regions are 2.5σ wide and are separated from the signal region by 3.5σ, where σ is the mass resolution determined from a fit of a single Gaussian to the D candidate mass spectrum.

The distribution of M^2_{rec}, summed over all $D\overline{D}$ channels, is shown in Fig. 2. The shaded histogram corresponds to the background in the signal region estimated from the $D\overline{D}$ mass sidebands. The small inset in Fig. 2

TABLE I: List of the reconstructed final states and corresponding values of efficiency times branching fraction.

Channel	First D decay mode	Second D decay mode	$\epsilon_i^{\mathcal{B}}(m_{D\overline{D}})$ $(\times 10^{-3})$
1. $D^0\overline{D}^0$	$D^0 \to K^-\pi^+$	$\overline{D}^0 \to K^+\pi^-$	0.14
2. $D^0\overline{D}^0$	$D^0 \to K^-\pi^+$	$\overline{D}^0 \to K^+\pi^-\pi^0$	0.42
3. $D^0\overline{D}^0$	$D^0 \to K^-\pi^+$	$\overline{D}^0 \to K^+\pi^-\pi^+\pi^-$	0.18
4. $D^0\overline{D}^0$	$D^0 \to K^-\pi^+\pi^0$	$\overline{D}^0 \to K^+\pi^-\pi^+\pi^-$	0.26
5. D^+D^-	$D^+ \to K^-\pi^+\pi^+$	$D^- \to K^+\pi^-\pi^-$	0.37
6. D^+D^-	$D^+ \to K^-\pi^+\pi^+$	$D^- \to K^+K^-\pi^-$	0.057
7. D^+D^-	$D^+ \to K^-\pi^+\pi^+$	$D^- \to K^0_S\pi^-$	0.042

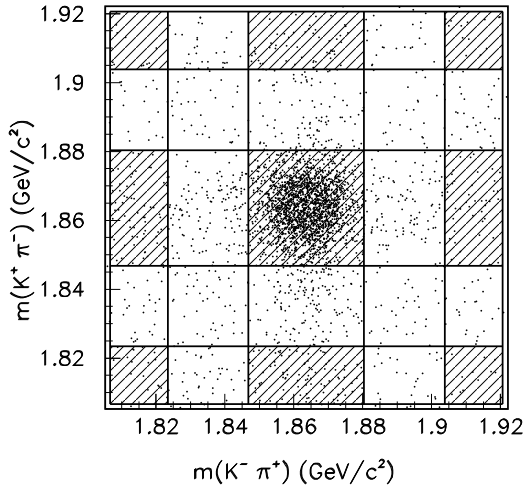

FIG. 1: $K^+\pi^-$ mass vs. $K^-\pi^+$ mass distribution for final state 1. The cross-hatched areas correspond to the signal and sideband regions.

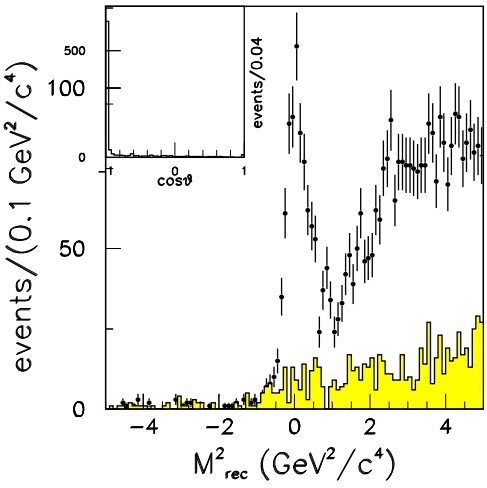

FIG. 2: Squared recoil mass, summed over all $D\overline{D}$ channels for ISR event candidates. The shaded histogram corresponds to non-$D\overline{D}$ background estimated from the $D\overline{D}$-mass sidebands. The small inset shows the distribution of the center-of-mass polar angle of the $D\overline{D}$ system in the ISR region.

shows the distribution of the $D\overline{D}$ center-of-mass polar angle θ for $D\overline{D}$ candidates with $\mid M^2_{rec} \mid < 1$ GeV$^2/c^4$. The sharp peak at $cos\theta = -1$ is typical of ISR production and agrees with Monte Carlo simulations.

The purity of each reconstructed D channel is demonstrated in Fig. 3 where projections of the candidate D mass distribution for events with $\mid M^2_{rec} \mid < 1$ GeV$^2/c^4$ are shown. Background is low in all channels.

The $D\overline{D}$ mass spectrum summed over all channels (860 events) is shown in Fig. 4 where the curves are the results from the fit described later. The shaded histogram represents the background determined using the $D\overline{D}$ sideband regions and corresponds to 17.5% and 7.1% of the signal candidates for $D^0\overline{D}^0$ and D^+D^-, respectively. We observe a clear $\psi(3770)$ signal and other structures at the positions of $\psi(4040)$ and $\psi(4415)$. We also observe a significant structure in the 3.9 GeV/c^2 region, which may not be due to a resonance; the coupled-channel model of Ref. [15] in fact describes qualitatively the observed $D\overline{D}$ mass spectrum and the structure around 3.9 GeV/c^2 without any need for additional ψ states.

To understand the background, we compute the expected contribution from ISR production of the $D^{*0}\bar{D}^0$ system. Using Monte Carlo simulations and the cross section estimate from Ref. [11] we find ≈ 6 % as possible contamination. This is confirmed by the examination of $D\gamma$ and $D\pi^0$ mass distributions where we find little evidence for D^{*0} signal. In contrast, strong evidence for D^{*0} production is observed for $M^2_{rec} > 1.5$ GeV$^2/c^4$. We investigate the possibility of background contributions from $D\overline{D}X$ final states (where $X \neq \gamma$) by exploring events in the M^2_{rec} sideband region $1.5 < M^2_{rec} < 2.5$ GeV$^2/c^4$. The $D\overline{D}$ mass spectrum for these events shows no structure. We conclude that the residual background

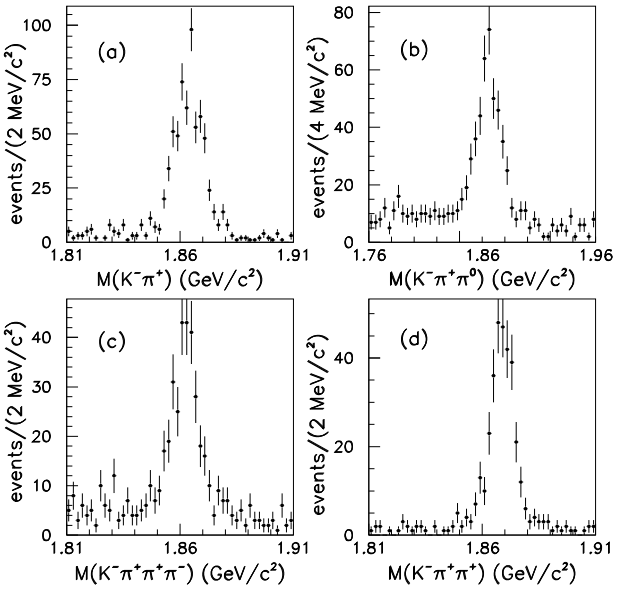

FIG. 3: D-candidate mass projections for events with $\mid M^2_{rec} \mid < 1$ GeV$^2/c^4$ and a $D\overline{D}$ invariant mass below 6 GeV/c^2. (a) $K^-\pi^+$ mass spectrum summed over channels 1, 2, and 3. (b) $K^-\pi^+\pi^0$ mass spectrum summed over channels 2 and 4. (c) $K^-\pi^+\pi^+\pi^-$ mass spectrum summed over channels 3 and 4. (d) $K^-\pi^+\pi^+$ mass spectrum for channel 5.

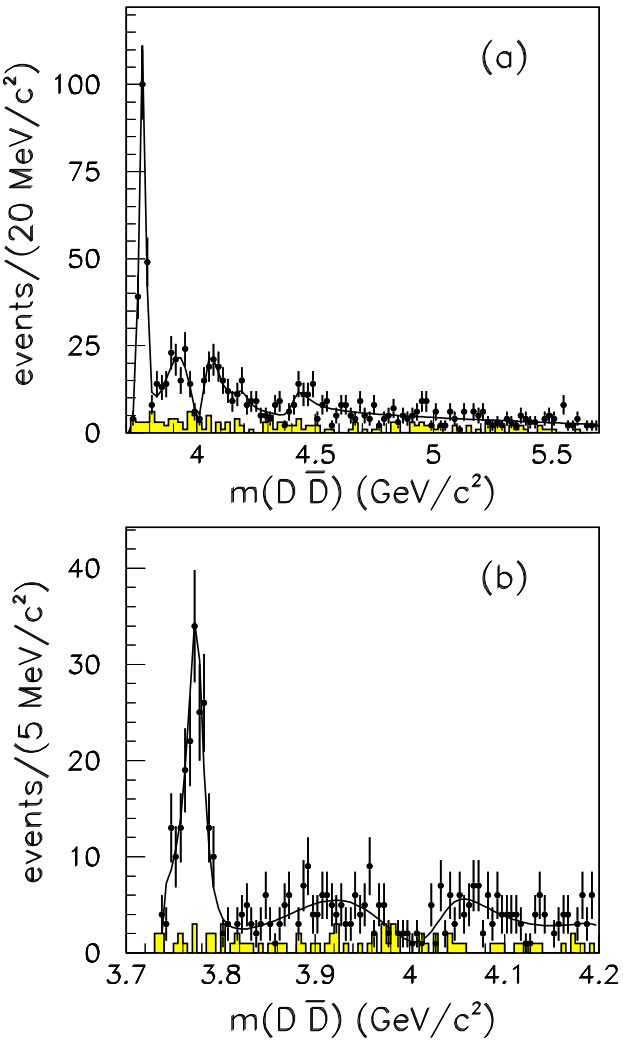

FIG. 4: (a) The ISR $D\overline{D}$ mass spectrum. The shaded mass spectrum is from $D\overline{D}$ mass sidebands. The curve results from the fit described in the text. (b) An expanded view of the region with $m_{D\overline{D}} < 4.2$ GeV/c^2.

to our signal is consistent with originating mostly from combinatorial non-$D\overline{D}$ events.

In order to measure efficiency and $D\overline{D}$ mass resolution, ISR events are simulated at eight different values of the $D\overline{D}$ invariant mass between 3.75 and 7.25 GeV/c^2. These events are generated using the GEANT4 detector simulation package [16] and are processed through the same reconstruction and analysis chain as are real events. The mass-dependent efficiency for each channel is fitted using a second-order polynomial. The mass resolution is determined from the difference between generated and reconstructed $D\overline{D}$ mass. The $D\overline{D}$ mass resolution is similar for all channels and increases with $D\overline{D}$ mass from 1.5 to 5 MeV/c^2. We observe good agreement between Monte Carlo and data M^2_{rec} distributions.

We define $N_i(m_{D\overline{D}})$ as the number of $D\overline{D}$ candidates for channel i. The channel branching fraction is $\mathcal{B}_i$, and $\epsilon_i(m_{D\overline{D}})$ is the efficiency as parametrized by the fitted polynomial. We define as $\epsilon_i^{\mathcal{B}}(m_{D\overline{D}})$ the product efficiency times branching fraction for each channel,

$$\epsilon_i^{\mathcal{B}}(m_{D\overline{D}}) = \epsilon_i(m_{D\overline{D}}) \times \mathcal{B}_i, \qquad (2)$$

and then compute $\epsilon^{\mathcal{B}}(m_{D\overline{D}})$ as

$$\epsilon^{\mathcal{B}}(m_{D\overline{D}}) = \frac{\sum_{i=1}^{7} N_i(m_{D\overline{D}})}{\sum_{i=1}^{7} \frac{N_i(m_{D\overline{D}})}{\epsilon_i^{\mathcal{B}}(m_{D\overline{D}})}}. \qquad (3)$$

The values of $\epsilon_i^{\mathcal{B}}(m_{D\overline{D}})$ are proportional to the expected yield for each channel. Their values, integrated over the $D\overline{D}$ mass spectrum, are reported in Table I. The resulting yields, corrected for efficiency and branching fractions, are found to be consistent within the errors.

The $D\overline{D}$ cross section is computed using

$$\sigma_{e^+e^-\to D\overline{D}}(m_{D\overline{D}}) = \frac{dN/dm_{D\overline{D}}}{\epsilon^{\mathcal{B}}(m_{D\overline{D}}) dL/dm_{D\overline{D}}}. \qquad (4)$$

The differential luminosity is computed as [17]

$$\frac{dL}{dm_{D\overline{D}}} = L\frac{2m_{D\overline{D}}}{s}\frac{\alpha}{\pi x}(\ln(s/m_e^2)-1)(2-2x+x^2), \quad (5)$$

where α is the fine-structure constant, $x = 1 - m^2_{D\overline{D}}/s$, s is the square of the e^+e^- center-of-mass energy, m_e is the electron mass, and L is the integrated luminosity of 384 fb^{-1}. The background-subtracted cross sections for $D^0\overline{D}^0$ and D^+D^-, averaged over 20 MeV/c^2 bins, are shown in Fig. 5.

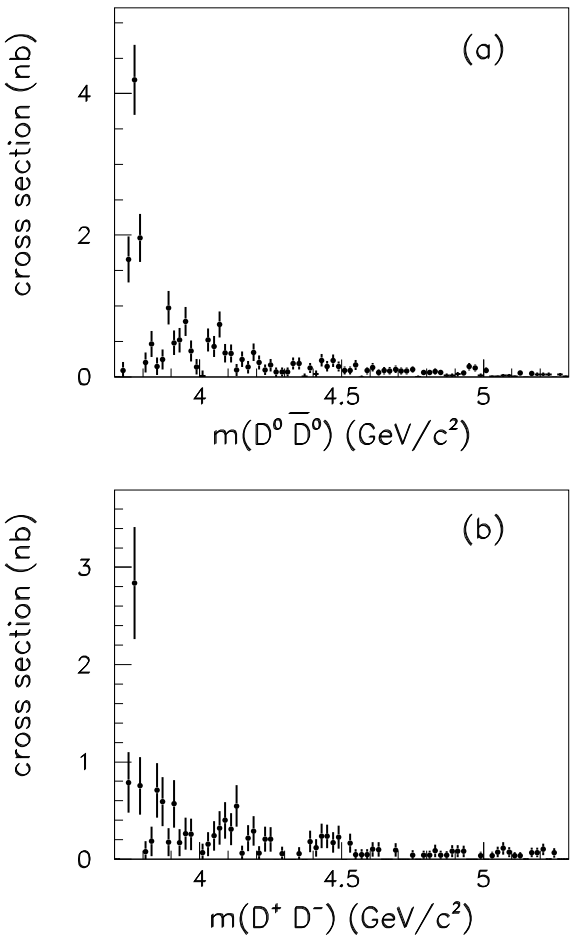

FIG. 5: (a) $D^0\overline{D}^0$ and (b) D^+D^- cross sections with statistical uncertainties only.

Systematic errors on the cross sections (10.9% for $D^0\overline{D}^0$ and 8.1% for D^+D^-) include uncertainties in the particle identification efficiencies and tracking efficiency, possible inaccuracies in the simulation of extraneous π^0 candidates, and uncertainties in the background estimates (≈ 6 %) and on the luminosity function (≈ 1 %).

Integrating the cross sections in the $\psi(3770)$ region (3.74-3.80 GeV/c^2), we compute the ratio of branching fractions,

$$\frac{\mathcal{B}(\psi(3770)\to D^0\overline{D}^0)}{\mathcal{B}(\psi(3770)\to D^+D^-)} = 1.78\pm0.33\pm0.24, \quad (6)$$

to be compared with the value of 1.28 ± 0.14 reported by the PDG [6].

We perform an unbinned maximum likelihood fit to the $D\overline{D}$ mass spectrum summed over all channels. The parameters of the $\psi(4040)$, $\psi(4160)$, and $\psi(4415)$ are fixed to the values reported in Ref. [18] while the $Y(4260)$ parameters are taken from our measurement from the $J/\psi\pi^+\pi^-$ channel [2]. The parameters of the $\psi(3770)$ are left free in the fit. In addition, we search for evidence of the $Y(4260)$ in this spectrum. Resolutions effects have been ignored since the widths of the resonances are much larger than the experimental resolution.

We express the total $D\overline{D}$ production as

$$f\left|P + c_1W_1e^{i\phi_1} + c_2\sqrt{G}e^{i\phi_2} + ... + c_nW_ne^{i\phi_n}\right|^2 + (1-f)B, \quad (7)$$

where c_i and ϕ_i are free parameters, W_i are spin-1 relativistic Breit-Wigner distributions, P represents the non-resonant contribution, B describes the non-$D\overline{D}$ background and f (0.829 ± 0.015) is the signal fraction. The efficiency $\epsilon^{\mathcal{B}}(m_{D\overline{D}})$ is almost linear and increases from $\approx 2\times10^{-3}$ to $\approx 4\times10^{-3}$ in the fitted mass region. It has been parametrized by a 2^{nd} order polynomial and it has been multiplied by P and W_i. The data require that we include the 3.9 GeV/c^2 structure, as suggested in Ref. [15], which we parameterize empirically as the square root of a Gaussian times a phase factor ($\sqrt{G}e^{i\phi_2}$). The parameters of the Gaussian are left free, and the phase allows interference with the ψ states.

We find that, in order to have a satisfactory description of the data, interference must be allowed between the resonances and the non-resonant contribution P. The latter contribution is parametrized either as a linear ($a+bm$) or a threshold function $(m-m_{th})^a e^{-bm-cm^2}$, where $m = m_{D\overline{D}}$, m_{th} is the threshold $D\overline{D}$ mass, and a, b and c are free parameters. This threshold function has also been used to describe the non-$D\overline{D}$ background B.

The two different parametrizations give similar results, which are considered in the evaluation of the systematic errors. These include also uncertainties in the D mass and on the overall $D\overline{D}$ mass scale. The size of the non-resonant production is determined by the fit.

The fit with a linear non-resonant contribution is shown in Fig. 4(a). Figure 4(b) shows an expanded view of the threshold region.

The fit returns the following parameters for the $G(3900)$ structure and for the $\psi(3770)$:

$$m(G(3900)) = (3943\pm17_{stat}\pm12_{syst})\,\mathrm{MeV}/c^2, \quad (8)$$

$$\sigma(G(3900)) = (52 \pm 8_{stat} \pm 7_{syst})\,\mathrm{MeV}/c^2, \quad (9)$$

$$m(\psi(3770)) = (3778.8 \pm 1.9_{stat} \pm 0.9_{syst})\,\mathrm{MeV}/c^2, \quad (10)$$

$$\Gamma(\psi(3770)) = (23.5 \pm 3.7_{stat} \pm 0.9_{syst})\,\mathrm{MeV}. \quad (11)$$

The systematic error on the $\psi(3770)$ mass includes uncertainties in the D mass, background parametrization, and detector related issues such as magnetic field, EMC corrections and energy loss. We measure a significantly higher $\psi(3770)$ mass with respect to previous measurements (3772.4±1.1) MeV/c^2 [6]. The change in likelihood due to the inclusion of a $Y(4260)$ amplitude in the fit is given by $\Delta(2\ln(L)) = 0.1$ with two additional fit parameters.

The systematic errors due to the masses and the widths of the $\psi(4040)$, $\psi(4160)$, $\psi(4415)$ and $Y(4260)$ resonances in the fit are evaluated by varying them by their statistical uncertainties. The signal fraction has been varied within its statistical error and the meson radius used in the Blatt-Weisskopf damping factor [19] present in the relativistic Breit-Wigner has been varied between 0 and 5 GeV^{-1}. The deviations from the central values are added in quadrature. The uncertainty on $\epsilon^{\mathcal{B}}(m_{D\overline{D}})$ is evaluated by using a weighted mean of branching fraction and efficiency uncertainties for the different channels. The fitted $Y(4260)$ yield before efficiency correction is $0.2 \pm 6.1_{stat} \pm 2.8_{syst}$ events.

This $Y(4260)$ yield in the $D\overline{D}$ channel is used to compute the cross section times branching fraction, which can then be compared to our measurement from the $J/\psi\pi^+\pi^-$ channel [2]. We obtain

$$\frac{\mathcal{B}(Y(4260) \to D\overline{D})}{\mathcal{B}(Y(4260) \to J/\psi\pi^+\pi^-)} < 1.0, \quad (12)$$

or

$$\Gamma(Y(4260) \to e^+e^-) \cdot \mathcal{B}(Y(4260) \to D\overline{D}) < 5.7\,\mathrm{eV}, \quad (13)$$

at 90% confidence level.

In conclusion, we have studied the exclusive ISR production of the $D\overline{D}$ system. The mass spectrum is dominated by $J^{PC} = 1^{--}$ states; in particular the $\psi(3770)$ is clearly seen. In order to fit the mass spectrum, signals from $\psi(4040)$, $\psi(4160)$, and $\psi(4415)$ have been included. The fit requires the presence of a broad structure near 3900 MeV/c^2. The presence of an enhancement in this region is predicted by a coupled channel model from Eichten *et al.* [15], although the possibility of the presence of a new ψ state cannot be excluded.

If the $Y(4260)$ is a 1^{--} charmonium state, it should decay predominantly to $D\overline{D}$ [4]; however no evidence is found for $Y(4260)$ decays to $D\overline{D}$. Other explanations have been proposed, such as a hybrid, baryonium, or tetraquark state.

We are grateful for the excellent luminosity and machine conditions provided by our PEP-II colleagues, and for the substantial dedicated effort from the computing organizations that support *BABAR*. The collaborating institutions wish to thank SLAC for its support and kind hospitality. This work is supported by DOE and NSF (USA), NSERC (Canada), CEA and CNRS-IN2P3 (France), BMBF and DFG (Germany), INFN (Italy), FOM (The Netherlands), NFR (Norway), MIST (Russia), MEC (Spain), and STFC (United Kingdom). Individuals have received support from the Marie Curie EIF (European Union) and the A. P. Sloan Foundation.

* Deceased
† Now at Tel Aviv University, Tel Aviv, 69978, Israel
‡ Also with Università di Perugia, Dipartimento di Fisica, Perugia, Italy
§ Also with Università della Basilicata, Potenza, Italy
¶ Also with Universitat de Barcelona, Facultat de Fisica, Departament ECM, E-08028 Barcelona, Spain

[1] S.-K. Choi *et al.*, Belle Collaboration, Phys. Rev. Lett. **91**, 262001 (2003).
[2] B. Aubert *et al.*, *BABAR* Collaboration, Phys. Rev. Lett. **95**, 142001 (2005).
[3] B. Aubert *et al.*, *BABAR* Collaboration, Phys. Rev. Lett. **98**, 212001 (2007); X.L. Wang *et al.*, Belle Collaboration, Phys. Rev. Lett. **99**, 142002 (2007).
[4] E.J. Eichten, K. Lane, and C. Quigg, Phys. Rev. **D73**, 014014 (2006).
[5] X.H. Mo *et al.*, Phys. Lett. **B640**, 182 (2006).
[6] W.-M.Yao *et al.*, Particle Data Group, Journal of Physics **G 33**, 1 (2006) and 2007 partial update.
[7] S. L. Zhu, Phys. Lett. **B625**, 212 (2005); E. Kou and O. Pene, Phys. Lett. **B631**, 164 (2005); F. E. Close and P. R. Page, Phys. Lett. **B628**, 215 (2005).
[8] L. Maiani, V. Riquer, F. Piccinini and A. D. Polosa, Phys. Rev. **D72**, 031502(R) (2005).
[9] X. Liu, X. Q. Zeng, and X. Q. Li, Phys. Rev. **D72**, 054023 (2005).
[10] E.S. Swanson, Phys. Rept. **429**, 243 (2006).
[11] G. Pakhlova *et al.*, Belle Collaboration, Phys. Rev. Lett. **98**, 092001 (2007).
[12] B. Aubert *et al.*, *BABAR* Collaboration, Nucl. Instrum. Methods **A479**, 1 (2002).
[13] Charge conjugate states are implied throughout this work.
[14] C. Cawlfield *et al.*, CLEO Collaboration, Phys. Rev. Lett. **98**, 092002 (2007).
[15] E. Eichten, K. Gottfried, T. Kinoshita, K.D. Lane, and T.M. Yan, Phys. Rev. **D21**, 203 (1980).
[16] S. Agostinelli *et al.*, GEANT Collaboration, Nucl. Instrum. Methods Phys. Res., Sect. A **506**, 250 (2003).
[17] M. Benayoun et al., Mod. Phys. Lett. **A14**, 2605 (1999).
[18] M. Ablikim *et al.*, BES Collaboration, arXiv:0705.4500 [hep-ex].
[19] J.M. Blatt and W.F. Weisskopf, Theoretical Nuclear Physics, John Wiley & Sons, New York, 1952.